2 × 2 Silicon Photonic MEMS Switch Based on Split Waveguide Crossing

Yinpeng Hu
State Key Laboratory for Modern Optical Instrumentation, College of Optical Science and Engineering, Zhejiang University
Hangzhou, China
yinpenghu@zju.edu.cn

Yi Sun
State Key Laboratory for Modern Optical Instrumentation, College of Optical Science and Engineering, Zhejiang University
Hangzhou, China
sy_borage@163.com

Ye Lu
State Key Laboratory for Modern Optical Instrumentation, College of Optical Science and Engineering, Zhejiang University
Hangzhou, China
lu_ye@zju.edu.cn

Huan Li*
State Key Laboratory for Modern Optical Instrumentation, College of Optical Science and Engineering, Zhejiang University
Hangzhou, China
lihuan20@zju.edu.cn

Daoxin Dai*
State Key Laboratory for Modern Optical Instrumentation, College of Optical Science and Engineering, Zhejiang University
Hangzhou, China
dxdai@zju.edu.cn

***Abstract*—We have proposed and implemented a novel 2 × 2 silicon photonic MEMS switch based on a split waveguide crossing, exhibiting experimentally low excess loss of 0.32 dB and high extinction ratio of 51 dB at 1550 nm.**

Keywords—Silicon photonics, MEMS, Optical switch, Reconfigurable network

I. Introduction

The current surge in cloud and data-intensive computing has resulted in an extensive growth of data centers, necessitating the development of large-scale photonic switches, which are crucial for the construction of reconfigurable networks. Although various silicon photonic switches based on micro-ring resonator (MRR) or Mach-Zehnder interferometer (MZI) using thermo-optic (TO) or electro-optic (EO) effects have been proposed in recent years[1-3], further scaling above port count of 32 [4, 5] remains a major challenge due to limitations such as high excess loss, high crosstalk, and sophisticated calibration procedures. To overcome these barriers, silicon photonic switches based on micro-electromechanical systems (MEMS) have been developed [6-10] and have realized up to 240 × 240 port counts with low excess loss (9.8 dB) and high extinction ratio (70 dB), while employing a digital switch operation to simplify the control strategy of the switch array. Nonetheless, these devices still suffer from fabrication compatibility issues as the vertical adiabatic coupler with two silicon layers requires customized foundry processes [11].

In this study, we present a novel 2 × 2 silicon photonic MEMS switch based on a split waveguide crossing (SWX) to achieve a compact footprint and large bandwidth. Our device is compatible with standard silicon photonics foundry processes and offers a potential solution to large-scale photonic switch arrays.

II. Structure and Design

The proposed switch is based on a SWX. When the two halves of the SWX are separated by a sufficiently large air gap, they effectively form two multimode waveguide corner-bends based on total internal reflection [12, 13], hence the input light turns 90° into the adjacent waveguide on the same side, and the switch is in its bar state, shown in Fig. 1(a). Meanwhile, when the two halves combine into one piece, they effectively form a multimode waveguide crossing based

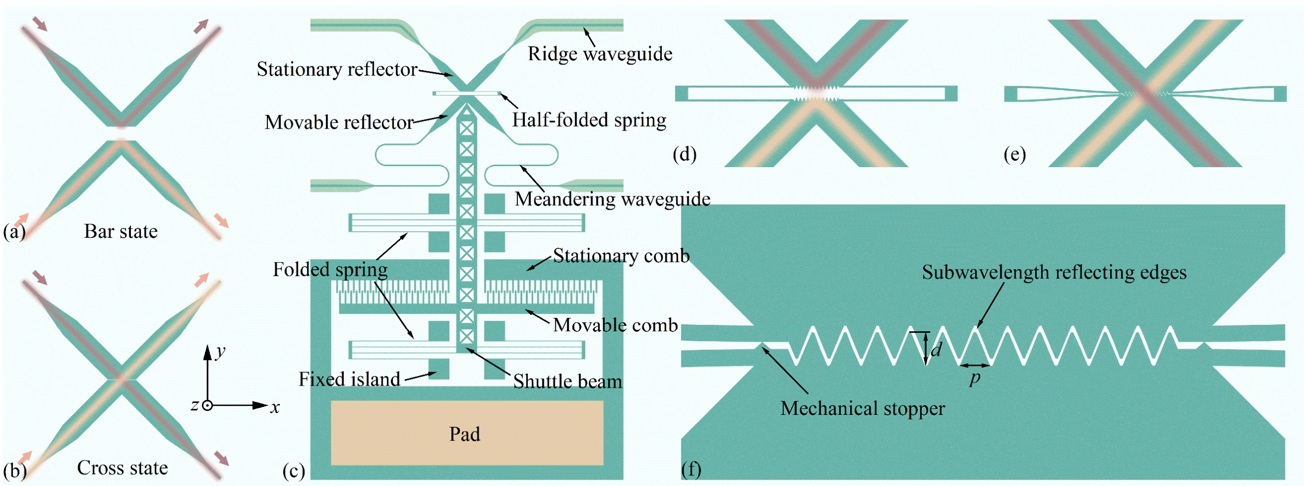

Fig. 1. Schematic diagram of the proposed device. Schematic diagram of the SWX in (a) bar state and (b) cross state, respectively. (c) Schematic diagram of the designed MEMS actuator. Schematic diagram of the SWX with SWT structures in (d) bar state and (e) cross state. (f) Close-up view of the SWT structures and the mechanical stoppers. *p* and *h* represent the period and depth of SWT, respectively.

on the self-imaging due to multimode interference, hence the input light propagates straight across, and the switch is in its cross state, shown in Fig. 1(b).

To achieve such operation principles, a MEMS actuator is designed to adjust the gap between the two SWX reflectors, as shown in Fig. 1(c), both of which are suspended. One of the SWX reflectors is fixed together with the ridge waveguide directly and is stationary, while the other reflector is movable due to the elastic deformation of the connected meandering waveguides. An electrostatic comb actuator is connected to the movable reflector through a shuttle beam along the y direction, which provides the driving force. Two pairs of folded springs are symmetrically connected to both sides of the shuttle beam to support the mechanical structures with valid flexibility. The two reflectors can be engaged and the device can be switched to cross state by increasing the actuator voltage, and when the voltage is removed, the device comes back to bar state due to the restoring forces of the springs and meandering waveguides that pull the movable reflector to its initial position. With the designed MEMS actuator, efficient and reliable switching function can be realized.

The proposed device described above is fabricated on a silicon-on-insulator (SOI) wafer with a 220-nm-thick top-silicon layer and a 2-µm-thick buried-oxide (BOX) layer. The SWX has a total length and width of 19.54 µm and 2.68 µm, respectively, and the taper waveguide is 6 µm in length. In the bar state, the initial gap between the two reflecting edges of the device is set to 1 µm to minimize crosstalk. In the cross state, direct contact between the reflecting edges must be avoided to prevent stiction. However, even a small gap between the reflecting edges can cause considerable reflection to the through port. To address this issue, mechanical stoppers and subwavelength teeth (SWT) structures are incorporated, as shown in Fig. 1(f). Two mechanical stoppers are introduced on the movable reflecting edge. Specifically, when the movable reflector approaches the stationary reflector, the tips of the mechanical stoppers contact the stationary reflecting edge first, which prevents further contact and minimizes the possibility of stiction. This contact also fixes the position of the movable reflector, which enables digital switching operation. Additionally, SWT structures are designed on the reflecting edges. The SWT structures on the two reflectors are complementary and can engage with each other tightly in the cross state, forming a refractive index gradient layer and increasing tolerance to the air gap. Width of the air gap between the engaged reflecting edges are precisely defined by the height of the mechanical stoppers. In our design, we choose p = 290 nm and d = 300 nm with 15-nm-height mechanical stoppers to obtain high extinction ratio in the cross state. The optimal design of the device is achieved using three-dimensional finite difference time domain (3D-FDTD) simulations. The simulated light propagation and transmission spectra are presented in Fig. 2, exhibiting 0.1–0.52 dB excess loss and 37.1–41.6 dB extinction ratio over the large bandwidth of 1400–1700 nm in the bar state and 0.09–0.46 dB excess loss and 22.5–24.1 dB extinction ratio over the same bandwidth in the cross state.

Elementary switches have been fabricated and tested as well. Fig. 3(a) shows the scanning electron microscope (SEM) image of the device. The photonic part (the SWX) has a footprint of 23 µm × 23 µm, while areas including the

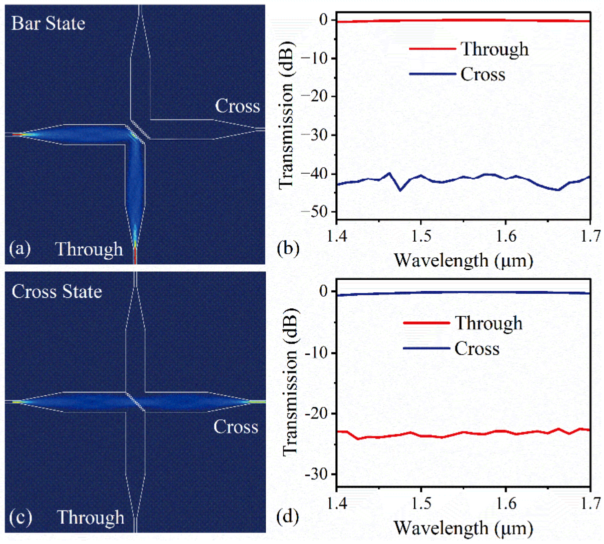

Fig. 2. Simulated light propagation and transmission spectra. (a)(b) Bar state. (c)(d) Cross state.Schematic diagram of the proposed device.

MEMS actuator is 95 µm ×100 µm. Fig. 3(b) provides a close-up view of the subwavelength teeth (SWT) and mechanical stopper, revealing a measurement of p = 290 nm and d = 285 nm. Amplified spontaneous emission (ASE) source and optical spectrum analyzer (OSA) were used to measure the device in the wavelength range of 1525–1575 nm for both switching states. The measured optical transmission spectra of the bar-state switch are presented in Fig. 3(c), which shows an excess loss and extinction ratio of < 0.67 dB and < 35 dB, respectively. Fig. 3(d) shows the measured optical transmission spectra of the cross-state switch, demonstrating an excess loss of < 1.1 dB and an extinction ratio of < 34 dB.

III. Conclusion

We have proposed and experimentally realized a novel 2 × 2 silicon photonic MEMS switch based on a split waveguide crossing (SWX). The operating principle of the device allows for a compact footprint, large bandwidth, and near-zero

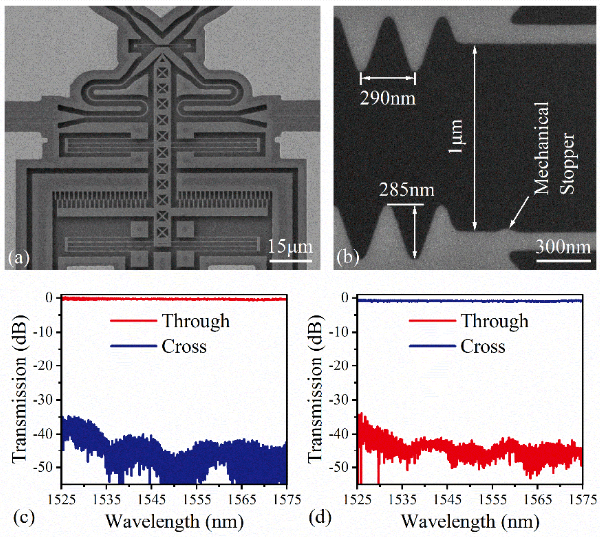

Fig. 3. Fabrication and measurement results. (a) SEM image of the device. (b) Close-up view of the SWT and mechanical stoppers. Measured transmission spectra of the device in (c) bar state and (d) cross state

power consumption. The device exhibits low excess loss of 0.11 dB in simulation and 0.32 dB in experiment at 1550 nm, combined with a high extinction ratio of 39 dB in simulation and 51 dB in experiment at 1550 nm. With the superiority mentioned above, large-scale optical switch arrays based on the proposed device can be realized and are expected to play critical roles in data centers.

ACKNOWLEDGMENT

This work is funded by Leading Innovative and Entrepreneur Team Introduction Program of Zhejiang (2021R01001), Zhejiang Provincial Major Research and Development Program (2021C01199), Natural Science Foundation of Zhejiang Province (LZ22F050006), and Startup Foundation for Hundred-Talent Program of Zhejiang University. The authors thank the ZJU Micro-Nano Fabrication Center and the Westlake Center for Micro/Nano Fabrication and Instrumentation for the facility support and technical assistance. The authors also acknowledge Tianjin H-Chip Technology Group Corporation for device fabrication.

REFERENCES

[1] W. Zhao, R. Liu, Y. Peng, X. Yi, H. Chen, and D. Dai, "High-performance silicon polarization switch based on a Mach–Zehnder interferometer integrated with polarization-dependent mode converters," *Nanophotonics,* vol. 11, no. 10, pp. 2293-2301, 2022, doi: doi:10.1515/nanoph-2022-0022.

[2] L. Song *et al.*, "Low-Loss Calibration-Free 2 × 2 Mach-Zehnder Switches With Varied-Width Multimode-Interference Couplers," *Journal of Lightwave Technology,* vol. 40, no. 15, pp. 5254-5259, 2022, doi: 10.1109/JLT.2022.3174133.

[3] S. Wang and D. Dai, "Polarization-insensitive 2 x 2 thermo-optic Mach-Zehnder switch on silicon," *Opt. Lett.,* vol. 43, no. 11, pp. 2531-2534, 2018/06/01 2018, doi: 10.1364/OL.43.002531.

[4] L. Qiao, W. Tang, and T. Chu, "32 × 32 silicon electro-optic switch with built-in monitors and balanced-status units," *Scientific Reports,* vol. 7, no. 1, p. 42306, 2017/02/09 2017, doi: 10.1038/srep42306.

[5] K. Suzuki *et al.*, "Low-Loss, Low-Crosstalk, and Large-Scale Optical Switch Based on Silicon Photonics," *Journal of Lightwave Technology,* vol. 38, no. 2, pp. 233-239, 2020, doi: 10.1109/JLT.2019.2934768.

[6] S. Han, T. J. Seok, N. Quack, B.-W. Yoo, and M. C. Wu, "Large-scale silicon photonic switches with movable directional couplers," *Optica,* vol. 2, no. 4, pp. 370-375, 2015/04/20 2015, doi: 10.1364/OPTICA.2.000370.

[7] T. J. Han S Fau - Seok, C.-K. Seok Tj Fau - Kim, R. S. Kim Ck Fau - Muller, M. C. Muller Rs Fau - Wu, and M. C. Wu, "Multicast silicon photonic MEMS switches with gap-adjustable directional couplers," (in eng), no. 1094-4087 (Electronic), 2015.

[8] T. J. Seok, N. Quack, S. Han, R. S. Muller, and M. C. Wu, "Large-scale broadband digital silicon photonic switches with vertical adiabatic couplers," *Optica,* vol. 3, no. 1, pp. 64-70, 2016/01/20 2016, doi: 10.1364/OPTICA.3.000064.

[9] S. Han, T. J. Seok, K. Yu, N. Quack, R. S. Muller, and M. C. Wu, "Large-Scale Polarization-Insensitive Silicon Photonic MEMS Switches," *Journal of Lightwave Technology,* vol. 36, no. 10, pp. 1824-1830, 2018, doi: 10.1109/JLT.2018.2791502.

[10] T. Nagai and K. Hane, "Silicon photonic microelectromechanical switch using lateral adiabatic waveguide couplers," *Opt. Express,* vol. 26, no. 26, pp. 33906-33917, 2018/12/24 2018, doi: 10.1364/OE.26.033906.

[11] T. J. Seok, K. Kwon, J. Henriksson, J. Luo, and M. Wu, "Wafer-scale silicon photonic switches beyond die size limit," *Optica,* vol. 6, p. 490, 04/20 2019, doi: 10.1364/OPTICA.6.000490.

[12] Y. Wang and D. Dai, "Multimode silicon photonic waveguide corner-bend," (in eng), *Opt Express,* vol. 28, no. 7, pp. 9062-9071, Mar 30 2020, doi: 10.1364/oe.387978.

[13] Y. Sun and D. Dai, "New concept of silicon photonic MEMS switch based on total internal reflection," in *2020 Asia Communications and Photonics Conference (ACP) and International Conference on Information Photonics and Optical Communications (IPOC)*, 24-27 Oct. 2020 2020, pp. 1-3.